Photon correlation studies of charge variation in a single GaAlAs quantum dot

B. Piętka,[1,2,*] J. Suffczyński,[1] M. Goryca,[1] T. Kazimierczuk,[1] A. Golnik,[1] P. Kossacki,[1] A. Wysmolek,[1] J. A. Gaj,[1,†] R. Stępniewski,[1] and M. Potemski[2]

[1]*Faculty of Physics, University of Warsaw, Warsaw, Poland*

[2]*Grenoble High Magnetic Field Laboratory, CNRS, Grenoble, France*

(Received 18 October 2012; revised manuscript received 6 January 2013; published 22 January 2013)

Complex charge variation processes in low-density, direct-type GaAlAs quantum dots embedded in a type-II GaAs/AlAs bilayer are studied by single-photon correlation measurements. Two groups of excitonic transitions are distinguished in the single quantum dot (QD) photoluminescence spectra, namely due to recombination of neutral and charged multiexcitonic complexes. The radiative cascades are found within each group. Three characteristic time scales are identified in the QD emission dynamics. The fastest one (of the order of 1 ns) is related to excitonic radiative recombination. The two remaining ones are related to the QD charge state variation. The one of 100-ns range (typical blinking time scale) corresponds to random capture of single carriers under a quasiresonant excitation. The slowest processes, in the range of seconds, are related to charge fluctuations in the surrounding of the dot.

DOI: 10.1103/PhysRevB.87.035310 PACS number(s): 78.55.Cr, 73.21.La, 71.35.−y

I. INTRODUCTION

A growing demand for few-electron, few-spin, and single-photon source devices has been stimulating the research on semiconductor quantum dots (QDs). These systems, with their characteristic discrete energy levels, are frequently referred to as artificial atoms. This analogy is supported by observations (common for atoms and QDs) of characteristic correlations (antibunching) between photons emitted from single objects.[1–5] Photon correlation experiments on single dots are also used to study their other properties, such as fluctuations of energy configuration of a dot and dynamics of optical excitation/recombination processes.[6–11] These latter effects are specific for the semiconductor environment of a QD, as opposed to an atom in vacuum. They are important for possible applications of the QD systems in optoelectronic devices.

We investigated correlations between photons emitted from a single quantum dot, focusing the attention on the effects of charge fluctuations and mechanisms of capture of photoexcited carriers. The dots show random temporal switching between two mutually excluding configurations, identified as their neutral and negatively charged state. When the excitation energy is high (above the barrier gap), the photoexcited electrons and holes are found to be captured separately by the dot. This results in a high probability of the QD charge state variation. In contrast, carriers are preferentially trapped in pairs (excitons) under quasiresonant, below-barrier excitation. Then, the characteristic switching time between the two charge configurations is found to be in the range of 100–10 ns, depending on the excitation power. The relative probability of finding the dot in a given configuration (relative intensity of corresponding emission lines) is seen fluctuating even on the time scale of seconds. These slow fluctuations can be tuned by the actual position of the laser spot with respect to the dot location. Our observations emphasize the importance of the actual semiconductor environment for the optical properties of quantum dots.

II. SAMPLE CHARACTERISTICS AND EXPERIMENTAL DETAILS

The active part of the structure used for experiments was intentionally designed as a type-II GaAs/AlAs bilayer ($d_{\mathrm{GaAs}} = 2.4$ nm, $d_{\mathrm{AlAs}} = 10$ nm) embedded between wide (100-nm) $Ga_{0.67}Al_{0.33}As$ barriers. The estimated characteristic band gaps of the bilayer (inset to Fig. 1) are $E_{\Gamma\text{-}X_{XY}} = 1.72$ eV (indirect gap involving the conduction band level of the X_{XY} symmetry in this particular structure) and $E_{\Gamma\text{-}\Gamma} = 1.75$ eV (direct band gap of the bilayer). However, the bilayer has been found to be significantly imperfect in lateral directions. We believe the bilayer imperfections consist of gallium-rich inclusions which can be described as $Ga_{1-x}Al_xAs$ islands. These direct gap islands, with remarkably low surface density of $\sim 10^6$ cm^{-2} and estimated lateral diameter of $\sim$50 nm, show spectroscopic properties typical of semiconductor QDs.[12–14] The QDs are strongly confined, as typically up to five/six fairly equidistant atomiclike shells,[15,16] separated by 8 to 20 meV, depending on the selected dot, are observed in photoluminescence (PL). The three-dimensional (3D) confinement is provided by $Ga_{0.67}Al_{0.33}As$ barriers in the direction of the growth and by the two-dimensional (2D) type-II GaAs/AlAs bilayer in the lateral direction.

The QD emission is distributed over a broad (approximately 160 meV) spectral range, below the energy of the indirect gap ($E_{\Gamma\text{-}X} = 1.72$ eV) of the surrounding GaAs/AlAs bilayer. The dots are efficiently excited at energies exceeding the direct band gap ($E_{\Gamma\text{-}\Gamma} = 1.75$ eV) of the GaAs/AlAs bilayer. Under such excitation, the photocarriers are predominantly created in the surrounding bilayer. After relaxation, they live long (approximately 1 ms) at the indirectly aligned X conduction and Γ valence band edges,[17] but are easily trapped into the dots, where they efficiently recombine.[14,18–20] When excitation is tuned below $E_{\Gamma\text{-}X}$ (and practically below $E_{\Gamma\text{-}\Gamma}$, as Γ-X absorption is very weak), the photocarriers are predominantly created directly in the dots.

Figure 1 shows typical micro-photoluminescence (μ-PL) spectra of a single QD at different excitation powers. For the

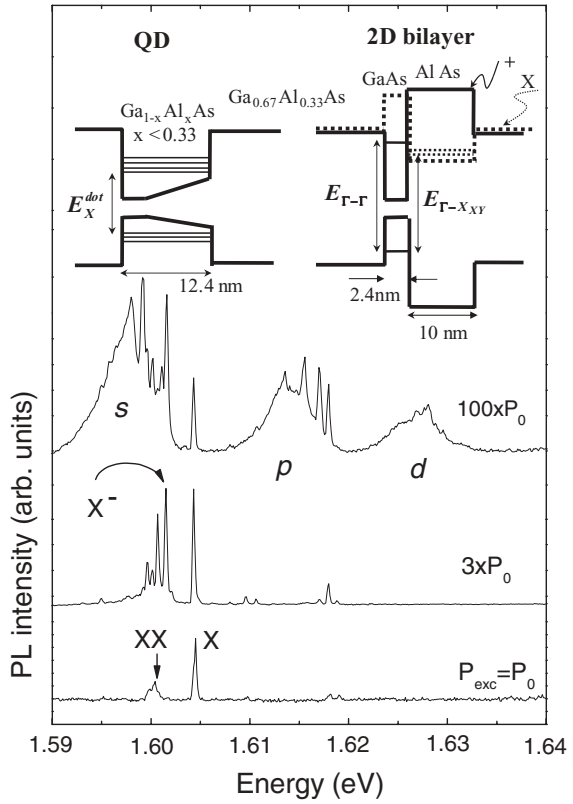

FIG. 1. Representative micro-PL spectra of our single QD at different intensities of quasiresonant excitation. The emission lines indicated as X, XX, and X^- are, respectively, due to exciton, biexciton, and negatively charged exciton recombination. The spectrum measured at the highest excitation power illustrates the recombination processes associated with s, p, and d confined shells of the dot. Inset: Scheme of the potential profile along the growth direction of the active part of the GaAs/AlAs type-II bilayer (right panel) and of the corresponding gallium-rich inclusions (left panel). Solid and dotted lines illustrate the states with Γ and X symmetry, respectively. Single excitons confined in our dots provide emission lines in the 1.56–1.72 eV energy range.

lowest excitation power (P_0), a dominant single emission line at 1.604 eV is observed. We attribute it to the simplest excitonic state, a single neutral exciton (X). At a higher excitation power ($3P_0$), the average number of carriers in the QD increases, and as a result additional emission lines emerge in the spectra: due to charged exciton (X^-) and biexciton (XX) recombination, at around 3 meV below the X emission. Eventually, at $100\times$ P_0, QD emission takes the form of a series of broad bands, marked as s, p, and d in Fig. 1. They correspond to a multiexcitonic recombination involving carriers confined in s, p, and d shells, respectively.[13] Arguments for the assumed identification of the observed excitonic transitions will be presented successively in the text.

Single-photon correlation experiments were performed under cw excitation in a Hanbury-Brown and Twiss configuration.[21,22] The signal from a single QD was sent through a 50/50 beam splitter to two grating monochromators (spectral resolution of 100 μeV each) tuned to a desired emission line. The filtered light was then detected by two avalanche photodiodes fixed at the outputs of the monochromators. The measurement yields a histogram of correlated photon pairs as a function of time separating detection of the first and the second photon in a pair. A negative value on the time axis of the histogram means that the first photon in the pair was detected on the "stop" and the second one on the "start" diode.

Two types of cw excitation were used. The first one was quasiresonant ($\hbar\omega_{\mathrm{exc}} \leqslant 1.726$ eV), below the quantum well (QW) indirect transition. It created electrons and holes directly in quantum dots. The second one was nonresonant ($\hbar\omega_{\mathrm{exc}} > 1.751$ eV), above the direct interband transition in the bilayer system. The nonresonant excitation generated efficiently electron-hole pairs, which were accumulating in the indirect quantum well and were subsequently relaxing to QDs.

III. EXCITATION INDUCED QD CHARGE STATE

For both types of excitations, a single-photon character of the excitonic emission from a single QD was demonstrated by a typical sharp antibunching dip at the zero delay time[3,4,23] ($\tau = 0$) in the X-X autocorrelation histogram. Figure 2(c) shows the respective histogram recorded for the case of quasiresonant excitation. The width of the antibunching dip is governed by the exciton lifetime, excitation rate, and the resolution of the setup (of the order of a nanosecond in our case).

Aside from the dynamics in the 1-ns time scale, related to radiative recombination of the QD exciton states, slower processes related to QD charge state variation can be also detected using correlation techniques. An observation of efficient cross correlation between the charged and the neutral exciton transitions is itself a proof of a significant rate of QD charge state variation. We were able to study these processes in a time scale extending from single nanoseconds to seconds.

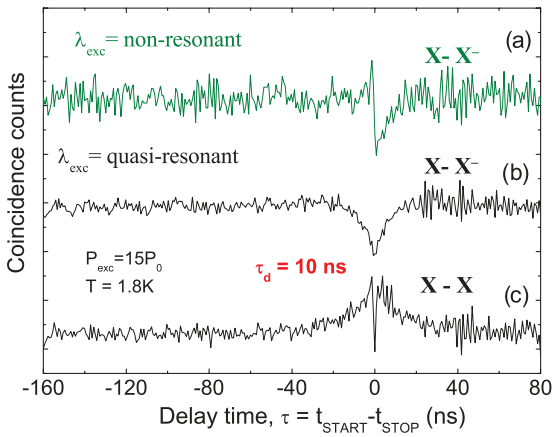

FIG. 2. (Color online) (a), (b) X-X^- cross-correlation histograms under nonresonant (above 1.75 eV, that is, above the QD barriers) and quasiresonant (below 1.75 eV, that is, below the QD barriers) excitation. (c) X-X photon correlation histogram for the same excitation power and excitation energy as (b). The same long-time-scale correlation evidenced in (b) and (c) histograms indicates that the QD state switches only between neutral and one type of charged configuration of carriers (corresponding to a majority carrier in X^-).

A. Nonresonant excitation

An X-X^- cross-correlation histogram, measured at nonresonant excitation, is shown in Fig. 2(a). It exhibits an expected deep minimum at zero delay and an asymmetric shape typical for neutral-charged exciton cross correlation:[6,7,21,24] a sharp peak at $\tau < 0$ and a slow rise for $\tau > 0$. The bunching peak at negative delays illustrates an increased probability of X-photon detection following emission of an X^- photon. Indeed, a reexcitation of the QD directly after the charged exciton recombination requires a single carrier to be trapped, while three carriers are necessary for the opposite emission order, resulting in the slow rise for $\tau > 0$. As discussed in Ref. 21, such asymmetric X-X^- histogram is observed when the single carrier capture is a dominant mechanism of the QD excitation. It is interesting to note here that even when the excitation occurs via the quantum well, which acts as a reservoir of indirect excitons, the quantum dot is trapping individual carriers. If the single carrier capture is suppressed, e.g., in case of the resonant excitation, we expect a different shape of the histogram, as discussed in the following.

B. Quasiresonant excitation

Figure 2(b) shows an X-X^- cross-correlation histogram, measured on the same QD as previously, but under the quasiresonant excitation. In contrast to the case of nonresonant excitation, the observed histogram is perfectly symmetric around the zero delay. The strong anticorrelation, observed at $\tau = 0$, decays at both negative and positive delay with a characteristic time of the order of tens of ns.

The observation of symmetric cross-correlation histogram indicates that in the case of resonant excitation, a probability of X^- after X detection is the same as the detection of X after the X^-. This means that the single carrier capture to the dot is inefficient, as expected when optical excitation supplies the carriers to the dot in pairs possessing no effective charge. This is different from the nonresonant excitation case, when a single particle left in the QD after the charged exciton recombination results in the increased probability of formation of the neutral exciton by simple trapping of a complementary carrier. The respective variation time of the QD charge state $1/\tau_d$ is found to be typically of the order of tens to hundreds of ns and to shorten with the increasing excitation power, as will be shown in the following.

The same long-time effects are visible in the autocorrelation histograms of neutral exciton photons [see Fig. 2(c)]. We observe an increased probability of detection of the second exciton photon after the first one was emitted, before a steady state is reached. This process is governed by the same relaxation time τ_d, as visible in Figs. 2(b) and 2(c). Similar symmetric histograms were already observed for autocorrelation of exciton photons emitted from resonantly excited InAs QDs (Ref. 11) and interpreted in terms of blinking effects in a two-level system.

The carrier dynamics in a QD under quasiresonant excitation is strongly modified by the excitation power. The X-X autocorrelation histograms, measured at different excitation powers, are presented in Fig. 3. It is found that the characteristic time τ_d varies from 400 to 15 ns when the excitation power is varied over an order of magnitude from $2 \times P_0$ to $15 \times P_0$. Similar dependencies were observed in X-X^- cross-correlation histograms (not shown). This shows that the quasiresonant excitation supplies not only charge-neutral carrier pairs to the dot as expected, but stimulates also non-negligible single carrier capture and/or removal processes and that a rate of these processes increases with the intensity of excitation.

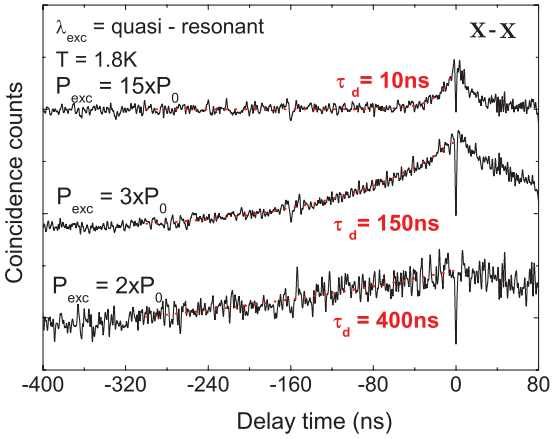

FIG. 3. (Color online) X-X autocorrelation histograms for different excitation powers taken at quasiresonant excitation. The dashed lines represent the fit with the exponential curve (Ref. 1): coincidence counts $(\tau) \sim g^{(2)}(\tau) \sim 1 - \exp(-\tau/\tau_d)$. The parameter $1/\tau_d$ represents the charge variation time in the investigated system.

The long-time effects in correlation histograms could be also considered as due to the bright to dark state transitions. However, it is not the case of this study as can be concluded from the X-X autocorrelation measurements at high excitation power. The X-X autocorrelation performed at the excitation power exceeding the saturation level (see Fig. 3) exhibits the blinking time scale much longer (∼10 ns) than the bright exciton lifetime (∼1 ns). Above the saturation level, excitons are captured to the dot with the periodicity that corresponds to the bright exciton lifetime. This shortens the lifetime of the dark exciton and would limit a time scale of blinking to a bright exciton lifetime of ∼1 ns, which we do not observe. Thus, we conclude that in our case the dark exciton state has minor contribution to the observed long-time-scale correlations.

IV. SELECTIVE CASCADES WITHIN NEUTRAL AND CHARGED STATES OF A QD

Multiexcitonic emission from the quantum dot is observed when many excitons simultaneously populate the dot. Single nth exciton recombination leaves the dot in $(n-1)$th multiexcitonic state. Due to the number of possible excitonic configurations in the initial and final states, the time-integrated emission spectrum is composed of a number of emission lines. Figure 4 illustrates a typical emission spectrum of the studied single dot excited with the power adjusted to populate only the ground s and first excited p shells. We have performed cross-correlation and autocorrelation measurements between most of the emission lines emerging in the spectrum (some examples are shown in Fig. 5).

All emission lines of the studied QD can be divided into two groups: the first one due to recombination of the neutral

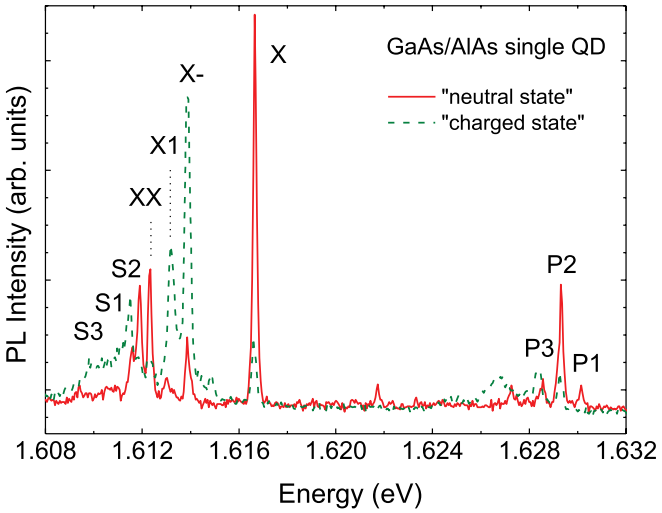

FIG. 4. (Color online) Typical emission spectra of a single GaAlAs quantum dot at moderate excitation power at quasiresonant excitation (a QD different than the one presented in Fig. 1). The emission of the QD switches between two sets of transitions, due to recombination of neutral (solid black line) and charged (dotted green line) QD states.

complexes X, XX, $S2$, and $P2$, and the second one due to recombination of the (negatively) charged complexes X^-, $X1, P3, P1, S1$. The cross-correlation histograms between the emission lines from two groups give a long-time anticorrelation effect, as for X-X^- [see Fig. 2(b)] and $X - X1$, X^--XX, $P2$-X^-, $P2$-$X1$, X^--$A2$, $X1$-$A2$, X-$S1$, X-$P1$ (see Fig. 5 for a few examples).

We have tested all sufficiently strong emission lines. We did not find any additional family of charged states that in experiment should give the long-time anticorrelation effects

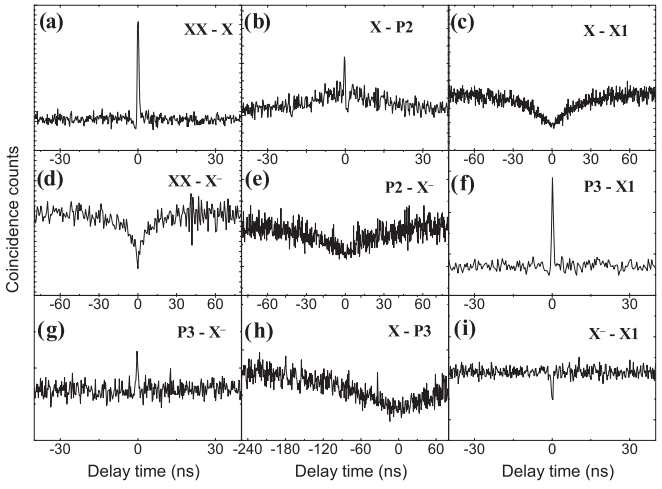

FIG. 5. The set of autohistograms and cross histograms of correlated counts as a function of time interval $\tau = \tau_{\mathrm{START}} - \tau_{\mathrm{STOP}}$ between photon registration events in start and stop detectors, tuned to indicated excitonic transitions as indicated in each panel (start-stop order). The corresponding emission lines are shown in Fig. 4. The unnormalized intensity scale is different for each histogram. Quasiresonant excitation was used.

with both X and X^- emissions. Thus, we can conclude that we observe only one type of charged state. We identify it as negative, taking into account the particular shape of the QD confining potential, significantly deeper for electrons than for holes. As the long-time anticorrelation effects observed in the histograms are typical for the emission lines originating from the states of different charge, the cross-correlation histograms performed within the family of the same charge are more complicated, composed mostly of the cascades. The cascaded recombination is only possible within one family of states.

In particular, we have observed the exciton (X) and biexciton (XX) recombination cascades [Fig. 5(a)]. The typical bunching[25] close to zero delay time means that shortly after the XX recombination, we observe the X recombination, before the ground state is reached. The particular asymmetry around zero delay time means that always the XX photon is emitted first and then the X photon can be detected. Thus, the XX recombination supplies the X state. The long-time-scale correlation effects are practically not visible in Fig. 5(a) since in order to avoid overlapping of the biexciton transition with other emission lines and to efficiently measure the XX-X cross correlation, we excite the QD with a very low excitation power (please refer to the PL spectra shown in Fig. 1). The cascade observed in the $P2$-X histogram [Fig. 5(b)] is more complicated in structure. The long-time positive correlation effect indicates that the two lines are due to recombination of two states of the same charge, with the $P2$ emission being initial. The antibunching dip is more pronounced than those in XX-X cascade, indicating that the recovery time after X emission is much longer.

Additionally, two other pronounced cascades are found between $P3$ and $X1$ lines, and between $P3$ and X^- [Figs. 5(g) and 5(f), respectively]. The asymmetry of the observed cascades around zero delay shows that in both cases the $P3$ emission is prior to the X^- or $X1$ recombination. However, to determine the nature of these sequenced emissions, more detailed analysis is needed. As already mentioned, all the emission lines $P3$, $X1$, and X^- are due to the charged state recombination. The $X1$-X^- correlation histogram shows sharp antibunching at exactly zero delay time, which indicates that the $X1$ and X^- emissions are due to two different excitonic states, not decaying subsequently within the same radiative cascade. At the same time, the origin of both states is due to the same higher excitonic state recombination as this is indicated by the observation of the $P3$-$X1$ and $P3$-X^- cascades. This means that X1 and X$^-$ are of the same charge and are composed of the same number of carriers, but they differ from each other by the carriers' electronic configuration. We can therefore assume that the $P3$ emission is due to the charged biexciton recombination as the most simple charged excitonic complex, the X^- and $X1$ being the same charged trion state recombination. The energy splitting between the X^- and $X1$ emission lines due to the additional charge carrier localized on excited p shell in the initial state (or in the final state the charge is left in excited state, which is much less probable). Possibly, these are the singlet and triplet trion states. This can be the case when the spin relaxation time of the carrier located at the p shell is longer than trion recombination time.

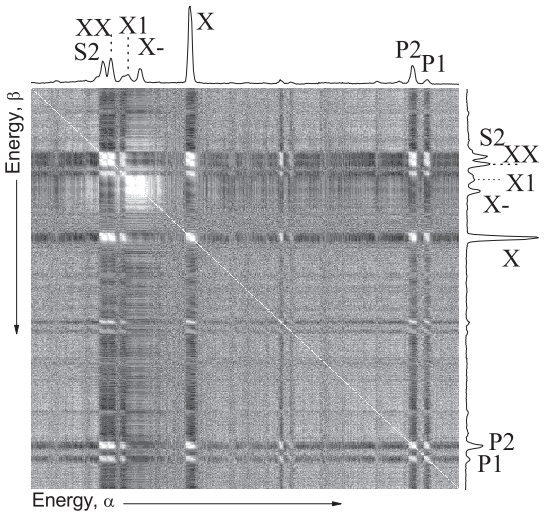

FIG. 6. Map of the Γ correlation coefficient matrix for a number of consecutively measured micro-PL spectra. The color scale illustrates positive $\Gamma = +1$ (white) and negative $\Gamma = -1$ (black) correlations, respectively. The average of all the recorded spectra is shown at the top and on the right-hand side of the map.

V. SWITCHING BETWEEN THE CHARGED AND NEUTRAL MULTIEXCITONIC STATES

As we have discussed above, the process of random switching of the QD charge state, being of the order of hundreds of nanoseconds, is sensitive to the excitation conditions, such as the excitation energy and power. In this section, we will show that this random switching is observable also in the time scale as large as a few seconds and that it is possible to switch the quantum dot from charged to neutral configuration and *vice versa* in a controllable manner.

In order to observe QD charge switching effects at large time scales, a number (a few hundreds) of PL spectra were taken one by one with the acquisition time of 1 s at constant excitation conditions. Figure 4 shows two μ-PL spectra of the QD (solid and dotted lines) with the smallest and the highest X emission intensity in the set. It is directly seen that each of the two spectra favors one of the group of excitonic transitions belonging to one of the two charge state "families" identified in the photon correlation measurements. A classical coefficient of the intensity correlation between intensities at different energies α and β in the PL spectrum provides an easy and powerful method of attributing transitions to different charge state group. This is calculated as

$$\Gamma = \frac{\sum_i \left(I_i^\alpha - \overline{I}^\alpha\right)\left(I_i^\beta - \overline{I}^\beta\right)}{\sqrt{\sum_i \left(I_i^\alpha - \overline{I}^\alpha\right)^2 \sum_i \left(I_i^\beta - \overline{I}^\beta\right)^2}}, \qquad (1)$$

where I_i^α, I_i^β are intensities of the signal in the spectrum i measured at energies α and β, respectively; $\overline{I}^\alpha$ and $\overline{I}^\beta$ are the average intensities over all spectra at energies α and β, respectively.[26] Figure 6 shows a calculated map of the coefficient Γ versus energies α (bottom/top scale) and β (right/left scale). Positive (up to $\Gamma = 1$) and negative (down to $\Gamma = -1$) correlated signals are found at the cross points of the emission lines in interest (at α and β energies). The map is symmetric versus the diagonal. The points on the diagonal represent a correlation of the intensity at given energy with itself, as expected, equal to 1. Let us take the neutral exciton X emission, as an example, to illustrate the method to read the correlation map. From the top QD spectrum above the map at the α X emission energy if one follows downwards (in the direction of the increasing β energy), the positive correlations are found at the β energies corresponding to the following emission lines: $S2, XX, X, P2, P1$. The same procedure can be applied to the whole spectrum. The map in Fig. 6 not only confirms the assignment of the excitonic emission lines to the two charge state families established previously, but reveals correlations at other energies, allowing one to extend this assignment.

A slight displacement of the laser spot (by less than 0.2 μm) on the sample surface is found to induce a variation of relative intensities of X and X^- emission lines by more than an order of magnitude. Similar blinking effects have already been reported.[1,4,6,11,27–29] They were discussed mainly in terms of Auger-type processes[1] and of the influence of impurities and/or defects in the vicinity of the QD.[6,28] We interpret the observed charge state variation as resulting from local electric fields created by charges of defect or impurity centers in the vicinity of the QD, fluctuating under influence of photoexcitation. These effects are also expected to be sensitive to local heating by the laser beam. Hence, by selecting the position of the excitation spot with respect to the QD, we are able to determine the average QD charge state and resulting QD emission pattern.

VI. SUMMARY

The particular type of GaAs/AlAs structure used in our experiments allowed us to observe a number of stable multiexcitonic states in a single quantum dot. We attributed the observed emission lines to neutral or negatively charged states of the QD. This classification was based on the observation of radiative cascades within each charge state "family." The dominant mechanism of the photoexcitation of the QD was determined from photon correlation measurements. It was found to be different depending on the excitation energy: single carrier capture in the case of nonresonant excitation in the AlAs barrier, or capture of entire excitons under quasiresonant excitation (below the barrier). However, even in the quasiresonant case, a blinking of the quantum dot between its two charge states was observed, with a characteristic time in a range from tens of nanoseconds to seconds, depending inversely on the excitation intensity. The average charge state of the QD is strongly affected by a displacement of the exciting laser spot with respect to QD position, even as small as 100 nm.

ACKNOWLEDGMENTS

This work was partially supported by the Polish Ministry of Science and Higher Education as research grants financed by Project No. MTKD-CT-2005-029671 and NCBiR project LIDER as well as by EuroMagNETII(JRA8) under the EU contract 228043. The samples were grown by Richard Planel at the L2M-CNRS Laboratory, Bagneux, France.

*barbara.pietka@fuw.edu.pl
†Deceased.

[1] P. Michler, A. Imamoğlu, M. D. Mason, P. J. Carson, G. F. Strouse, and S. K. Buratto, Nature (London) **406**, 968 (2000).
[2] V. Zwiller, H. Blom, P. Jonsson, N. Panev, S. Jeppesen, T. Tsegaye, E. Goobar, M.-E. Pistol, L. Samuelson, and G. Bjork, Appl. Phys. Lett. **78**, 2476 (2001).
[3] P. Michler, A. Kiraz, C. Becher, W. V. Schoenfeld, P. M. Petroff, L. Zhang, E. Hu, and A. Imamoğlu, Science **290**, 2282 (2000).
[4] C. Santori, M. Pelton, G. Solomon, Y. Dale, and Y. Yamamoto, Phys. Rev. Lett. **86**, 1502 (2001).
[5] Z. Yuan, B. Kardynal, R. Stevenson, A. Shields, C. Lobo, K. Cooper, N. Beattie, D. Ritchie, and M. Pepper, Science **295**, 102 (2002).
[6] A. Kiraz, S. Falth, C. Becher, B. Gayral, W. V. Schoenfeld, P. M. Petroff, L. Zhang, E. Hu, and A. Imamoğlu, Phys. Rev. B **65**, 161303 (2002).
[7] M. H. Baier, A. Malko, E. Pelucchi, D. Y. Oberli, and E. Kapon, Phys. Rev. B **73**, 205321 (2006).
[8] S. M. Ulrich, M. Benyoucef, P. Michler, N. Baer, P. Gartner, F. Jahnke, M. Schwab, H. Kurtze, M. Bayer, S. Fafard, Z. Wasilewski, and A. Forchel, Phys. Rev. B **71**, 235328 (2005).
[9] P. Dalgarno, J. McFarlane, D. Bruner, R. Lambert, B. Gerardot, R. Warbuton, K. Karrai, A. Badolato, and P. Petroff, Appl. Phys. Lett. **92**, 193103 (2008).
[10] J. Suffczyński, K. Kowalik, T. Kazimierczuk, A. Trajnerowicz, M. Goryca, P. Kossacki, A. Golnik, M. Nawrocki, J. A. Gaj, and G. Karczewski, Phys. Rev. B **77**, 245306 (2008).
[11] C. Santori, D. Fattal, J. Vučković, G. S. Solomon, E. Waks, and Y. Yamamoto, Phys. Rev. B **69**, 205324 (2004).
[12] B. Piętka, Ph.D. thesis, Joseph Fourier University, Grenoble I, France and University of Warsaw, Warsaw, Poland, 2007.
[13] B. Chwalisz, A. Wysmolek, R. Stępniewski, M. Potemski, S. Raymond, R. Bozek, and V. Thierry-Mieg, Int. J. Mod. Phys. B **21**, 1654 (2007).
[14] M. D. Martín, C. Antón, L. Viña, B. Piętka, and M. Potemski, Europhys. Lett. **100**, 67006 (2012).
[15] S. Raymond, S. Studenikin, A. Sachrajda, Z. Wasilewski, S. J. Cheng, W. Sheng, P. Hawrylak, A. Babinski, M. Potemski, G. Ortner, and M. Bayer, Phys. Rev. Lett. **92**, 187402 (2004).
[16] A. Babiński, M. Potemski, S. Raymond, J. Lapointe, and Z. R. Wasilewski, Phys. Rev. B **74**, 155301 (2006).
[17] A. Wysmolek, B. Chwalisz, M. Potemski, R. Stępniewski, A. Babiński, S. Raymond, and V. Thierry-Mieg, Acta Phys. Pol. A **106**, 367 (2004).
[18] A. Wysmolek, M. Potemski, and V. Thierry-Mieg, Physica E (Amsterdam) **12**, 876 (2002).
[19] B. Chwalisz, A. Wysmolek, R. Stępniewski, A. Babiński, M. Potemski, and V. T. Mieg, Int. J. Mod. Phys. B **18**, 3807 (2004).
[20] J. Suffczyński, A. Trajnerowicz, T. Kazimierczuk, B. Piętka, K. Kowalik, P. Kossacki, A. Golnik, M. Nawrocki, J. A. Gaj, A. Wysmolek, R. Stępniewski, M. Potemski, and V. Thierry-Mieg, Acta Phys. Pol. A **112**, 461 (2007).
[21] J. Suffczyński, T. Kazimierczuk, M. Goryca, B. Piechal, A. Trajnerowicz, K. Kowalik, P. Kossacki, A. Golnik, K. P. Korona, M. Nawrocki, J. A. Gaj, and G. Karczewski, Phys. Rev. B **74**, 085319 (2006).
[22] R. Hanbury-Brown and R. Q. Twist, Nature (London) **178**, 1447 (1956).
[23] D. V. Regelman, U. Mizrahi, D. Gershoni, E. Ehrenfreund, W. V. Schoenfeld, and P. M. Petroff, Phys. Rev. Lett. **87**, 257401 (2001).
[24] A. Malko, M. Baier, E. Pelucchi, D. Chek-al-kar, D. Oberli, and E. Kapon, Physica E (Amsterdam) **26**, 194 (2005).
[25] E. Moreau, I. Robert, L. Manin, V. Thierry-Mieg, J. M. Gerard, and I. Abram, Phys. Rev. Lett. **87**, 183601 (2001).
[26] Before calculating the correlation map the spectra were normalized, thus, the total emission intensity of each spectrum was the same. As a result, the dark anticorrelation regions appear in the map when exciton emission is correlated with a background. The assumed procedure assures, however, that the positive correlations are better pronounced in the map.
[27] D. Bertram, M. C. Hanna, and A. J. Noizk, Appl. Phys. Lett. **74**, 2666 (1999).
[28] M.-E. Pistol, P. Castrillo, D. Hessman, J. A. Prieto, and L. Samuelson, Phys. Rev. B **59**, 10725 (1999).
[29] H. D. Robinson and B. B. Goldberg, Phys. Rev. B **61**, R5086 (2000).